

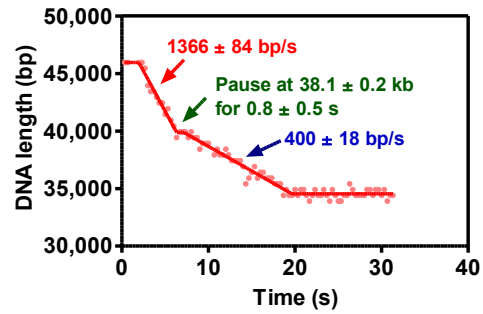
SUPPLEMENTARY INFORMATION

DNA Unwinding Heterogeneity by RecBCD Results from Static Molecules able to Equilibrate

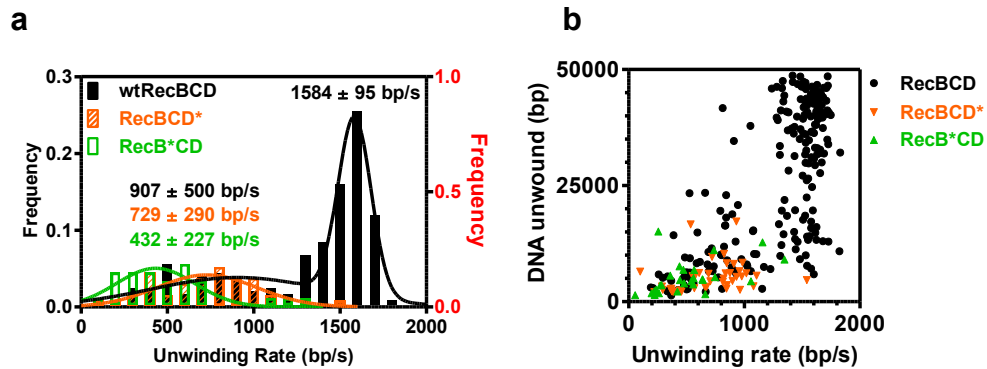
Bian Liu^{1,2,3}, Ronald J. Baskin², and Stephen C. Kowalczykowski^{1,2,3,*}

¹Department of Microbiology and Molecular Genetics, ²Department of Molecular and Cellular
Biology, ³Biophysics Graduate Group
University of California, Davis, California 95616

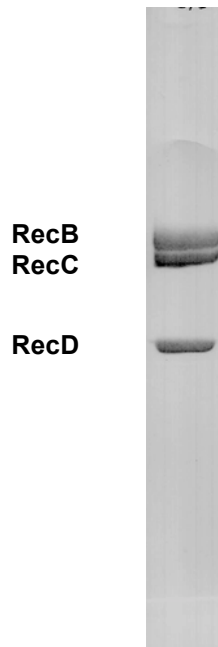
*Correspondence: Stephen C. Kowalczykowski, University of California, Department of
Microbiology and Molecular Genetics, One Shields Ave., Briggs Hall - Rm. 310, Davis, CA
95616-8665, Phone: 530-752-5938, Fax: 530-752-5939 E-mail: sckowalczykowski@ucdavis.edu



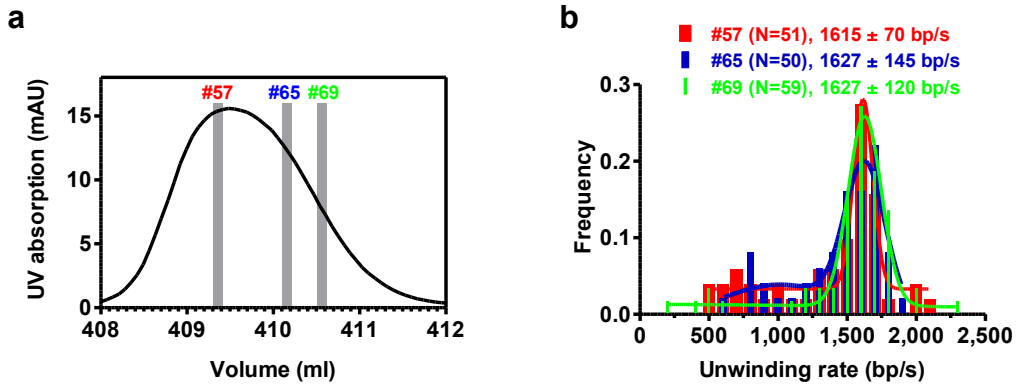
Supplementary Figure 1. An example of an event that resulted in a rate change during DNA unwinding by RecBCD. This is a representative time course showing a RecBCD molecule that reduced its unwinding rate on lambda phage DNA lacking a χ sequence. The length of DNA versus time was fitted to a continuous five-segment line using least-square fitting. Only 4% of the molecules showed such behavior, and thus, cannot account for the slow population in the velocity distribution of RecBCD enzyme (Figure 1).



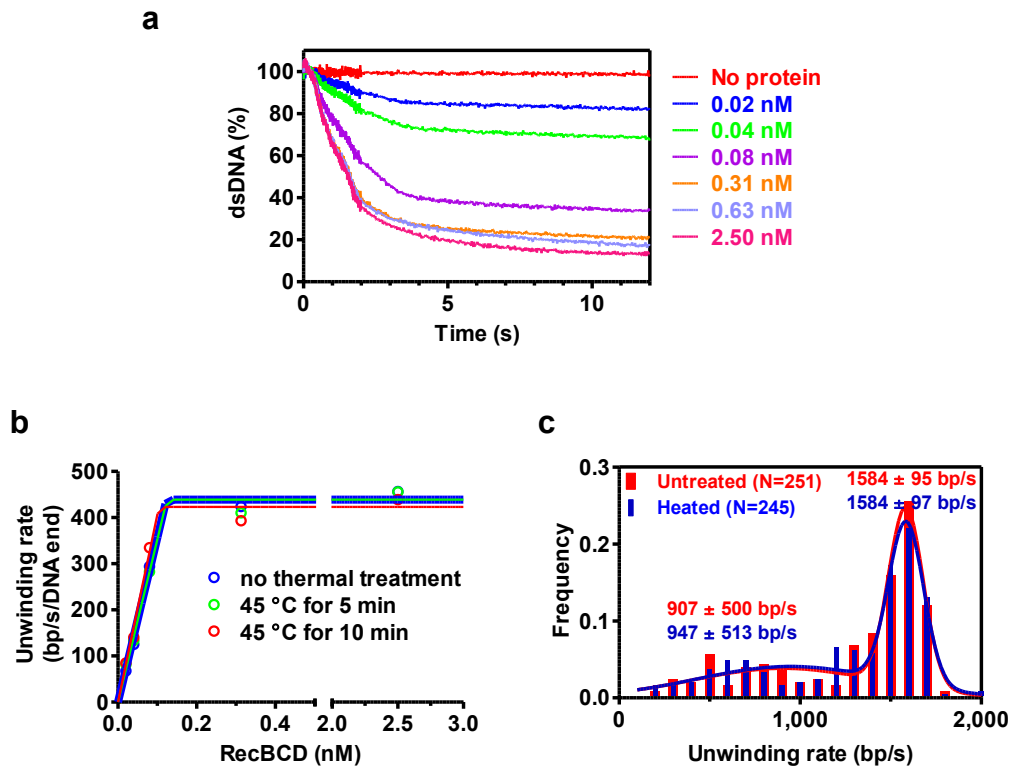
Supplementary Figure 2. The RecBCD molecules that are unwinding DNA comprise two populations. **a**, The slow population has an unwinding rate comparable to the single-motor mutants of RecBCD. The mean unwinding rate of RecBCD^{K177Q} is 729 ± 290 bp/s and that of RecB^{K29Q}CD is 432 ± 227 bp/s. **b**, The processivities of the two motor mutants, RecBCD^{K177Q} and RecB^{K29Q}CD, are 5.3 ± 3.4 kb and 5.1 ± 3.5 kb, respectively. The processivity of the major faster population of wild type RecBCD enzymes is 27.8 kb, which is in agreement with previous studies (~30 kb)^{4,7,10}; the processivity of the slower population overlays considerably with the distribution of the single-motor mutants, suggesting that either the RecB or RecD motor is not engaged in this group of RecBCD enzymes.



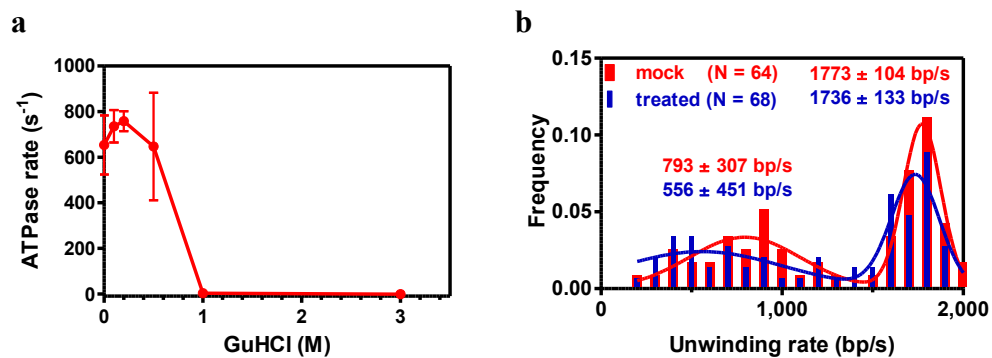
Supplementary Figure 3. The purified RecBCD is biochemically homogeneous. Shown is a Coomassie blue-stained 12% SDS-polyacrylamide gel of purified RecBCD (1 μ g). The positions of RecB, RecC, and RecD subunits are shown.



Supplementary Figure 4. Different chromatographic fractions of RecBCD enzyme have similar helicase activity. **a**, The UV absorption spectrum of RecBCD eluted in a salt gradient from a MonoQ column. The three grey bars showed the positions of the three fractions examined using single-molecule analysis. **b**, The distribution of unwinding rates for RecBCD enzymes in each fraction. The data were fitted to the sum of two Gaussian functions; however, the first peak was deemed “ambiguous” by the fitting software, and is not reported here. The mean of each second peak is 1615 ± 49 bp/s, 1627 ± 27 bp/s, and 1627 ± 10 bp/s (\pm SE) and the standard deviation is 70 ± 74 bp/s, 146 ± 38 bp/s, 120 ± 11 bp/s (\pm SE) for fraction #57 (red; N = 51), #65 (blue; N = 50) and #69 (green; N = 59), respectively. The tail probability (two-sample Kolmogorov-Smirnov distribution test) that the distributions of two samples are the same is: $P = 0.64$ for fraction #57 and #65; $P = 0.15$ for #57 and #69; $P = 0.23$ for #65 and #69.

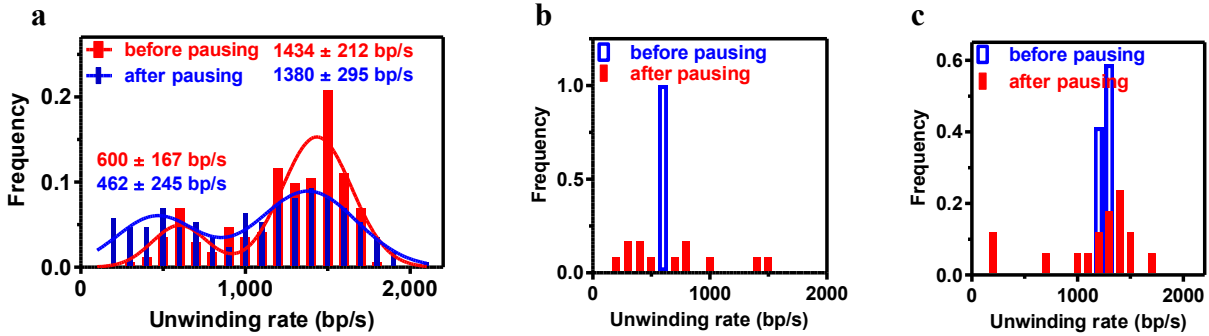


Supplementary Figure 5. Thermal annealing does not change the distribution of single-molecule unwinding rates. **a**, Example traces from the stopped-flow dye-displacement assay showing unwinding of DNA observed as a decrease in fluorescence due to displacement of Hoechst dye that was bound to the dsDNA. The traces shown are for untreated RecBCD enzyme. The final concentration of RecBCD after mixing is indicated. **b**, Protein titration showing that heating RecBCD at 45 °C for 5 or 10 min followed by slow cooling did not change its specific helicase activity. **c**, The distribution of unwinding rates for thermally treated RecBCD enzyme (blue; N = 245) versus untreated (red; N = 251; the same data as in **Fig. 1b**). The data are binned with 100 bp/s intervals and fitted to the sum of two Gaussian functions. For the treated enzyme, the mean of the first peak is 947 ± 122 bp/s (\pm SE) with SD = 513 ± 122 bp/s. The means of the second peak is 1584 ± 7 bp/s (\pm SE) with SD = 97 ± 9 bp/s.

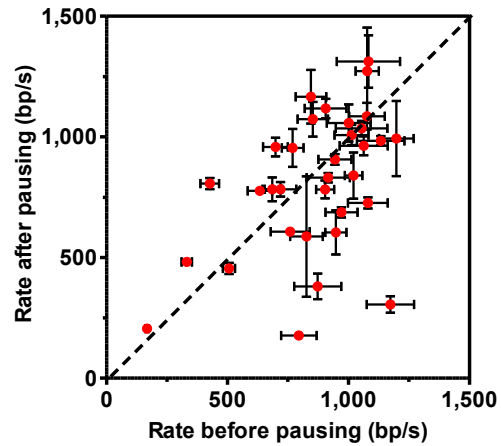


Supplementary Figure 6. Partial chemical unfolding does not change the distribution of

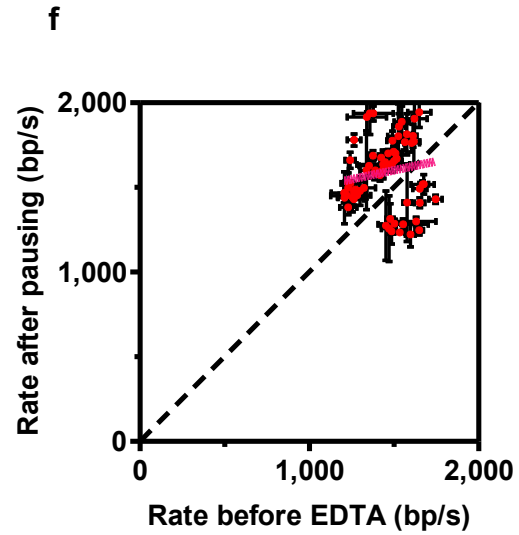
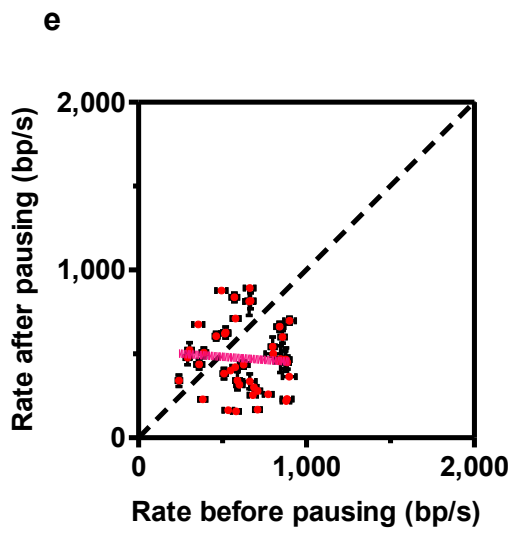
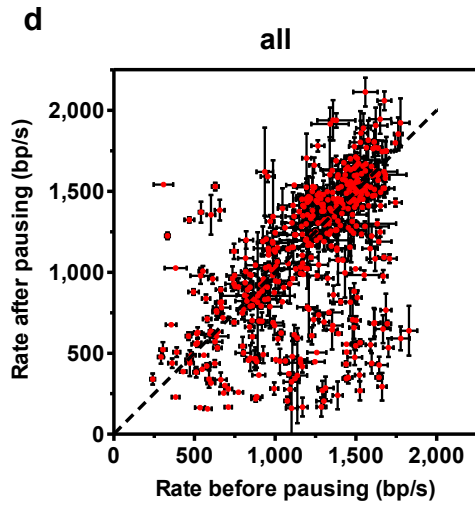
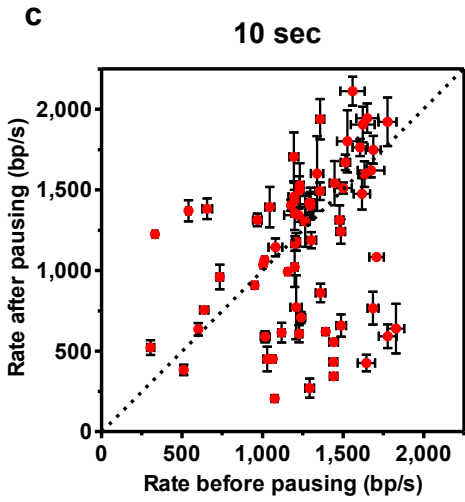
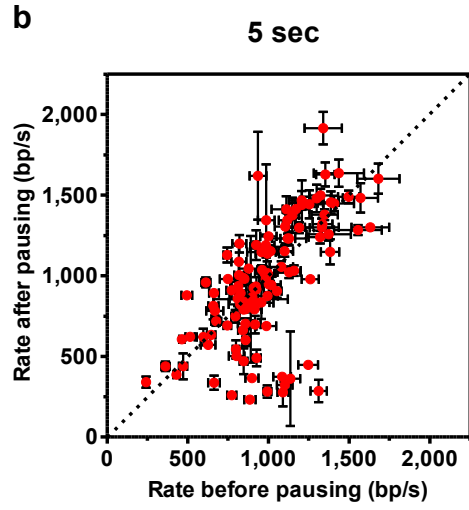
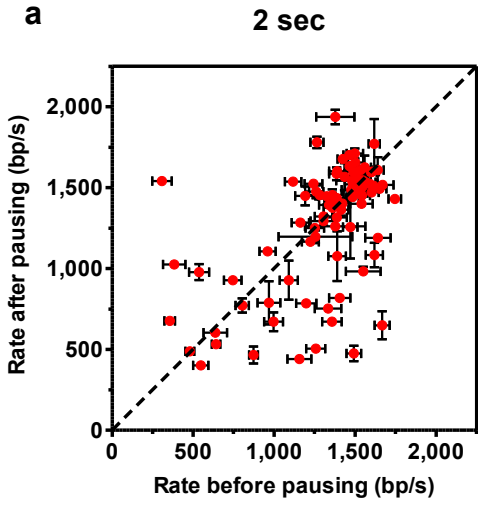
unwinding rates. a, The ATP hydrolysis rates of RecBCD treated with various concentrations of GuHCl followed by dialysis against B100 buffer. Data shown are the average value for two observations with the standard deviation as error bars. Mock- and GuHCl-treated RecBCD were further examined using single-molecule analysis. **b**, The distribution of unwinding rates for RecBCD enzymes treated with 0.5 M GuHCl (blue; N = 68) versus mocked-treated (red; N = 64). The data are binned in 100 bp/s intervals and fitted to the sum of two Gaussian functions. For the control enzymes, the mean of the first peak is 793 ± 49 bp/s (\pm SE) with SD = 307 ± 51 bp/s. The mean of the second peak is 1773 ± 9 bp/s (\pm SE) with SD = 104 ± 9 bp/s. For the enzymes treated with 0.5 M GuHCl, the mean of the first peak is 556 ± 177 bp/s (\pm SE) with SD = 451 ± 209 bp/s. The mean of the second peak is 1736 ± 21 bp/s (\pm SE) with SD = 133 ± 21 bp/s.



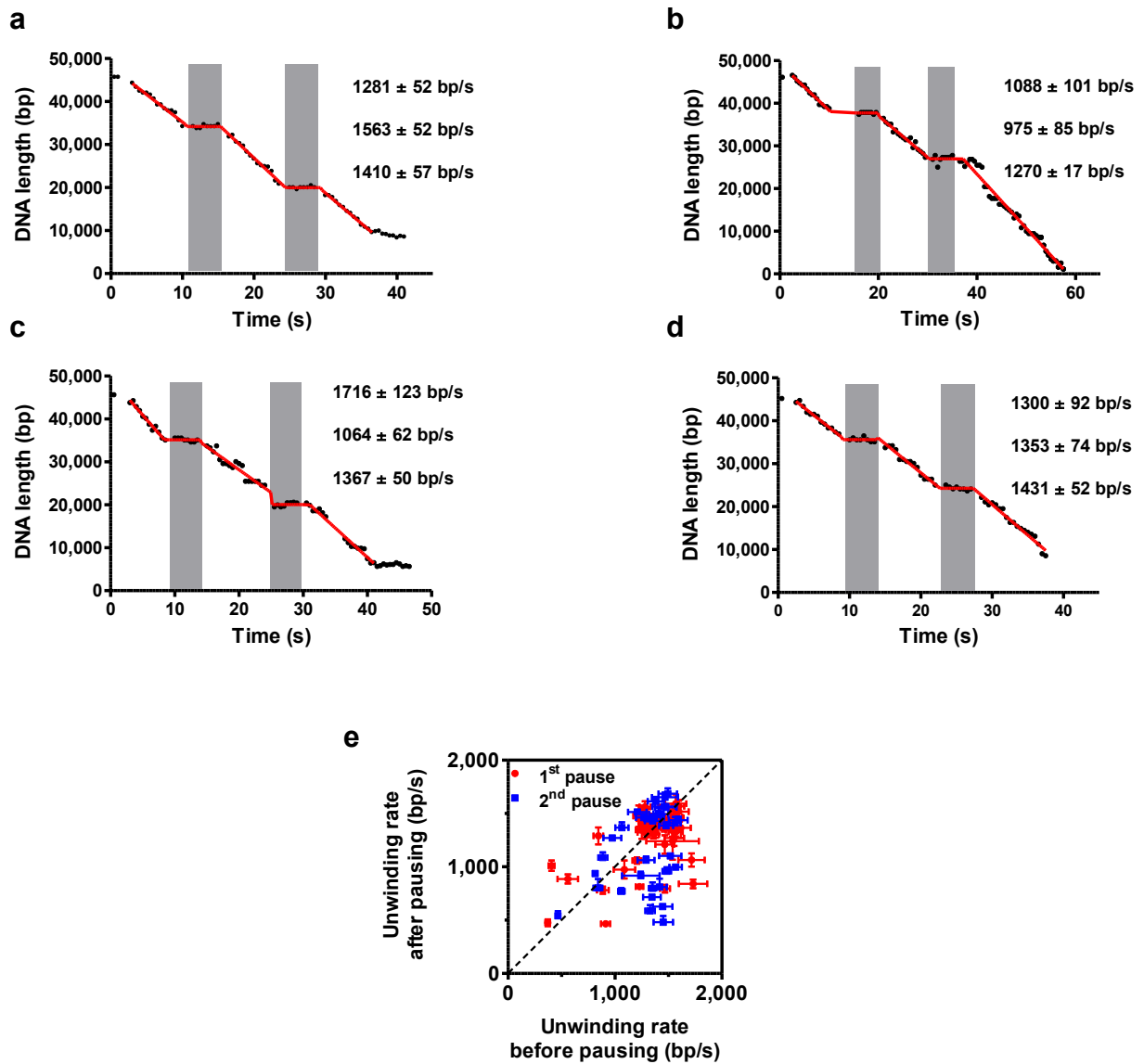
Supplementary Figure 7. Distribution of the unwinding rates before and after a 20-second incubation in the EDTA channel. a, The rates are grouped in 100 bp/s bins. The lines are least-square fits to the sum of two Gaussian functions; $N = 173$. Note that the mean of the slow unwinding group before pausing by EDTA was fixed at 600 bp/s to permit convergence in the fitting. **b**, Distribution of rates before (blue) and after (red) pausing for molecules with an initial rate between 550 and 650 bp/s ($N = 12$). **c**, Distribution of rates before (blue) and after (red) pausing for molecules with an initial rate between 1150 and 1350 bp/s ($N = 17$); before pausing, the selected bin from the original population had a mean velocity of 1259 ± 30 bp/s (SD); after pausing and redistribution, mean is 1168 ± 422 bp/s (SD) (median = 1331 bp/s). The mean and median values show that there is no correlation between the initial and final velocities. The mean velocities after pausing is, within error, the same as that of the original population average prior to pausing, which for Figure 2b is 1245 bp/s (SD ± 359 , $N = 173$; median = 1347 bp/s).



Supplementary Figure 8. Transiently stopping the enzyme by incubation for 5 seconds in the absence of ATP, but in the presence of Mg^{2+} , results in a similar effect on the rates as incubation in buffer containing EDTA. The rates before and after pausing are shown. $N = 33$. The error bars represent the error of the least-square fitting.



Supplementary Figure 9. The distribution of rates before and after pausing in EDTA channel for 2, 5, and 10 seconds and for all molecules. (a-c), Rates for 2, 5, and 10 second pauses. The proportion of molecules that changed rate by more than 20% is 33%, 39%, and 49% for a pause of 2 s (N = 87), 5 s (N = 116), and 10 s (N = 69), respectively. The fraction of molecules that changed rate in the 10 s and 20 s pausing experiments is significantly different from the number in the 2 s pause ($P < 0.05$; Fisher's exact test). **d,** Rates for all molecules (2, 5, 10, and 20 sec pauses; N = 445). The molecules that lie along the diagonal did not detectably change rate; for molecules that changed rate by more than 20% (N = 186), a linear fit yields a slope = 0.19 ± 0.09 ($P = 0.03$) and a Spearman correlation coefficient of 0.15 ($P = 0.04$) showing little or no correlation of rates prior to and after the ATP-depletion induced pause. **e and f,** Data analyzed in two separate groups to examine switching only within macrostates: in **e**, only the slow molecules (i.e., with only one motor attached) that switched only into another slow microstate are shown; included are those molecules whose speed was less than 900 bp/s, and that switched only into a state whose speed was also less than 900 bp/s; a linear fit yields a slope = -0.07 ± 0.17 ($P = 0.66$) and a Spearman correlation coefficient of 0.12 ($P = 0.43$) showing no correlation of rates prior to and after the pause induced by ATP-depletion. **f,** only the fast molecules (i.e., with both motors attached) that switched speed only into a fast microstate are shown; included are molecules whose speed was 1200 bp/s or greater, and that switched to a state whose speed was also 1200 bp/s or greater; a linear fit yields a slope = 0.21 ± 0.18 ($P = 0.24$) and a Spearman correlation coefficient of 0.15 ($P = 0.22$) showing no correlation of rates prior to and after the pause induced by ATP-depletion.



Supplementary Figure 10. The changes in rate for a single RecBCD molecule are not correlated when the molecule is paused multiple times. In this experiment, the bead-DNA-RecBCD complexes were dipped into the EDTA-channel twice. The traces were fit to multiple-segment line. **(a-d)** Representative traces showing the rates of four RecBCD enzyme molecules during the multiple-pausing protocol. Three rates are shown for each molecule: the first is the rate before pausing; the 2nd is the rate after the 1st pause; and the 3rd is the rate after the 2nd pause. The errors are the error of the least-square fitting. **e**, Scatter plot of the rates before and after each pausing. N = 34. The error bars are the error of the least-square fitting.